Synthesis, Crystal Structure, Spectral Studies, and Catechol Oxidase Activity of Trigonal Bipyramidal Cu(II) Complexes Derived from a Tetradentate Diamide Bisbenzimidazole Ligand

Manisha Gupta,[†] Pavan Mathur,*[,†] and Ray J. Butcher[‡]

Department of Chemistry, University of Delhi, Delhi-110007, India, and Department of Chemistry, Howard University, Washington, D.C. 20059

Received March 21, 2000

A new benzimidazole-based diamide ligand—*N*,*N*′-bis(glycine-2- benzimidazolyl)hexanediamide (GBHA)—has been synthesized and utilized to prepare Cu(II) complexes of general composition [Cu(GBHA)X]X, where X is an exogenous anionic ligand ($X = Cl^-$, NO_3^-, SCN^-). The X-ray structure of one of the complexes, [Cu(GBHA)Cl]Cl·H_2O·CH_3OH, has been obtained. The compound crystallizes in the monoclinic space group *C*2/*c* with unit cell dimensions $a = 26.464(3)$ Å, $b = 10.2210(8)$ Å, $c = 20.444(2)$ Å, $\alpha = 90°$, $\beta = 106.554(7)°$, $\gamma = 90°$, $V = 5300.7(9)$ Å^3, and $Z = 8$. To the best of our knowledge, the [Cu(GBHA)Cl]Cl·H_2O·CH_3OH complex is the first structurally characterized mononuclear trigonal bipyramidal copper(II) bisbenzimidazole diamide complex having coordinated amide carbonyl oxygen. The coordination geometry around the Cu(II) ion is distorted trigonal bipyramidal ($\tau = 0.59$). Two carbonyl oxygen atoms and a chlorine atom form the equatorial plane, while the two benzimidazole imine nitrogen atoms occupy the axial positions. The geometry of the Cu(II) center in the solid state is not preserved in DMSO solution, changing to square pyramidal, as suggested by the low-temperature EPR data $g_{\|} > g_{\perp} > 2.0023$. All the complexes display a quasi-reversible redox wave due to the Cu(II)/Cu(I) reduction process. $E_{1/2}$ values shift anodically from $Cl^- < NO_3^- < SCN^-$, indicating that the bound Cl^- ion stabilizes the Cu(II) ion while the N-bonded SCN^- ion destabilizes the Cu(II) state in the complex. When calculated against NHE, the redox potentials turn out to be quite positive as compared to other copper(II) benzimidazole bound complexes (Nakao, Y.; Onoda, M.; Sakurai, T.; Nakahara, A.; Kinoshita, L.; Ooi, S. *Inorg. Chim. Acta* **1988**, *151*, 55. Addison, A. W.; Hendricks, H. M. J.; Reedijk, J.; Thompson, L. K. *Inorg. Chem*. **1981**, *20* (1), 103. Sivagnanam, U.; Palaniandavar, M. *J. Chem. Soc., Dalton Trans*. **1994**, 2277. Palaniandavar, M.; Pandiyan, T.; Laxminarayan, M.; Manohar, H. *J. Chem. Soc., Dalton Trans*. **1995**, 457. Sakurai, T.; Oi, H.; Nakahara, A. *Inorg. Chim. Acta* **1984**, *92*, 131). It is therefore concluded that binding of amide carbonyl oxygen destabilizes the Cu(II) state. The complex [Cu^{II}(GBHA)(NO_3)](NO_3) could be successfully reduced by the addition of dihydroxybenzenes to the corresponding [Cu^{I}(GBHA)](NO_3). ^{1}H NMR of the reduced complex shows slightly broadened and shifted ^{1}H signals. The reduction of the Cu(II) complex presumably occurs with the corresponding $2e^-$ oxidation of the quinol to quinone. Such a conversion is reminiscent of the functioning of a copper-containing catechol oxidase from sweet potatoes and the *met* form of the enzyme tyrosinase.

Introduction

Tyrosinase is a copper-containing enzyme that contains two Cu(II) ions coupled via a magnetic exchange interaction. This coupled dinuclear copper(II) site is also the resting state of the enzyme and is referred to as *met*-tyrosinase.[1] The enzyme functions via a deoxy site which has two copper ions in the +1 oxidation state. An oxytyrosinase form is generated when the deoxy site reacts with molecular oxygen. The oxytyrosinase hydroxylates monophenols to diphenols and in turn produces the *met*-tyrosinase form containing two copper(II) ions. It is the *met*-tyrosinase form which is then further involved in the oxidation of diphenols to quinones, regenerating the deoxy site (Figure 1). This activity of *met*-tyrosinase is similar to that of catechol oxidase from sweet potatoes.[2]

The fact that in tyrosinase substrate binding to the copper center requires a rearrangement of a tetragonal copper site toward a trigonal bipyramidal arrangement[3] and the knowledge that copper centers in tyrosinase and catechol oxidase are bound by imidazole nitrogen of histidines prompted us to generate Cu(II) compounds having an intermediate geometry between

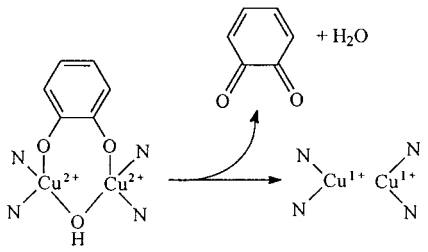

Figure 1. Proposed mechanism[23] for the oxidation of catechol by tyrosinase.

* To whom correspondence should be addressed at the University of Delhi.
[†] University of Delhi.
[‡] Howard University.

(1) Solomon, E. I.; Baldwin, M. J.; Lowery, M. D. *Chem. Rev*. **1992**, *92*, 521.
(2) Klabunde, T.; Eicken, C.; Sacchettini, J.; Krebs, B. *Nat. Struct. Biol*. **1998**, *5*, 1084.
(3) Wilcox, D. E.; Porras, A. G.; Hwang, Y. T.; Lerch, K.; Winkler, M. E.; Solomon, E. I.. *J. Am. Chem. Soc*. **1985**, *107*, 4015.

10.1021/ic000313v CCC: $20.00
Published on Web 01/23/2001

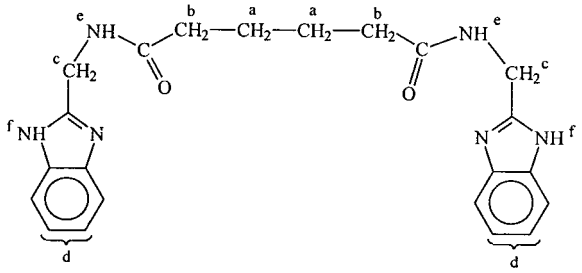

Figure 2. GBHA.

trigonal bipyramidal and square pyramidal in a nitrogen−oxygen donor environment. With this view in mind we have synthesized a tetradentate diamide ligand carrying pendant benzimidazole groups—*N*,*N*′-bis(glycine-2-benzimidazolyl)hexanediamide (GBHA) (Figure 2)—a ligating system that we are reporting for the first time.

Experimental Section

Materials. Glycinebenzimidazole dihydrochloride was prepared following the procedure reported by Cescon and Day.[4] Adipic acid was recrystallized from 50% nitric acid. Solvents were freshly distilled off prior to use. All other chemicals were obtained from commercial sources and were used as received. Catechol was twice sublimed on a coldfinger (mp 106 °C).

Physical Measurements. Elemental analyses were obtained from the microanalytical laboratory of RSIC, Chandigarh, India. Electronic spectra were recorded on a Beckman DU-64 UV/vis spectrophotometer (errors in UV/vis wavelength maxima are ±1 and ±4 nm, respectively). IR spectra were recorded in the solid state as KBr pellets on a Perkin-Elmer FTIR-2000 spectrometer (IR stretching frequencies measured to an accuracy of ±1 cm^{-1}). Magnetic susceptibilities of the complexes were determined using a vibrating sample magnetometer at 298 K in the solid state at USIC, Roorkee, India (error bar ±0.05 μ_B). Cyclic voltammetric measurements were carried out using a BAS CV 50W electrochemical analyzing system ($E_{1/2}$ measured to an accuracy of ±1.0 mV). Cyclic voltammograms of all the complexes were recorded in 2:8 DMSO−acetonitrile solutions, with 0.1 M $NaClO_4$ as supporting electrolyte. A three-electrode configuration composed of a Pt disk working electrode (3.1 mm^2 area), a Pt wire counter electrode, and a $Ag/AgNO_3$ reference electrode was used for the measurements. The reversible one-electron Fc^+/Fc couple in the above solvent system has an $E_{1/2}$ of 0.093 V vs a $Ag/AgNO_3$ electrode. (The $Ag/AgNO_3$ electrode itself is 0.557 V positive as compared to NHE.) X-band EPR spectra were recorded on a Varian E-112 spectrometer with a variable-temperature liquid nitrogen cryostat at IIT, Madras, India (the error in g values is ±0.01). ^1H NMR spectra were recorded on a 300 MHz Bruker-Spin instrument. X-ray diffraction data were collected by standard methods using graphite-monochromated Mo x-radiation at the Department of Chemistry, Howard University. All nonequivalent reflection intensities for which $3.8° < 2\theta < 60°$ were collected. The intensities of 3 standard reflections monitored every 97 reflections showed no greater fluctuations from Poisson statistics. The raw intensity data were corrected for Lorenz polarization effects and absorption.[5] The structure was solved by conventional Patterson and Fourier methods. A three-dimensional Patterson synthesis was used to determine the heavy atom positions which phased the data sufficiently well to permit the location of the remaining non-hydrogen atoms from difference Fourier synthesis. Values for scattering factors and anomalous dispersion terms (real and imaginary) were from standard sources.[6] Tests for extinction showed none significant. Full-matrix least-squares refinement of the model was carried out as described previously.[7] The hydrogen atoms were added in idealized positions in a "riding" model (i.e., when the atoms to which they are attached moved, during refinement their positions were recalculated in idealized geometry) with refined isotropic temperature factors. Further difference Fourier calculation enabled the location of the hydrogen atom positions, which were included in the refinement for four least-squares cycles and then held fixed. The model converged with an agreement factor of $R_{int} = 0.038$. A final Fourier difference map was featureless. Crystal data, positional parameters, and molecular matrixes are summarized in Tables1−3, respectively.

Synthesis of Ligand *N*,*N*′-Bis(glycine-2-benzimidazolyl)hexanediamide. The ligand was prepared following the procedure reported by Vagg et al.[8] To a solution of adipic acid (1.67 g, 11.4 mmol) in pyridine (20 mL) was added a solution of glycinebenzimidazole dihydrochloride (5.0 g, 22.8 mmol) in pyridine (30 mL). The mixture was stirred gently for 10 min, during which a white precipitate appeared. The reaction mixture was then heated slowly on a water bath at a temperature of 40 °C, and to it was added triphenyl phosphite (7.08 mL, 22.8 mmol) dropwise over a period of 15 min. The reaction mixture was simultaneously stirred. After addition of $P(OPh)_3$ was complete and the initially formed white precipitate dissolved, the temperature of the reaction mixture was slowly raised to 75 °C and the clear solution was stirred for 1 h. A white solid resulted which was filtered off, washed with chloroform, and neutralized. The white crystalline product so obtained was recrystallized with a EtOH−H_2O (1:2) mixture and analyzed for composition $C_{22}H_{24}N_6O_2 \cdot H_2O$. Anal. Found (Calcd): C, 61.95 (62.56); H, 6.14 (6.16); N, 19.73 (19.90). Mp 276 °C. Yield 1.9 g (41.1%). ^1H NMR (d_6-DMSO): δ (ppm) = 1.65 (quin, 4H), 2.26 (t, 4H), 4.54 (d, 4H), 7.15−7.49 (m, 8H), 8.44 (t, $2H_{amide\ NH}$), 12.07 (s, br, $2H_{benzim\ NH}$). IR (KBr pellets): 3296 cm^{-1} ($\nu_{N-H\ amide}$), 3185 cm^{-1} ($\nu_{N-H\ benzim}$), 1635 cm^{-1} ($\nu_{C=O\ amide\ I}$), 1539 cm^{-1}($\nu_{C-N\ amide\ II}$), 1448 cm^{-1} ($\nu_{C=N-C=C\ benzim}$). λ_{max}, nm (log ϵ) (MeOH): 243 (3.67), 272 (3.68), 279 (3.68).

Synthesis of the Complexes. [CuCl(GBHA)]Cl·H_2O·CH_3OH. To a methanolic solution of $CuCl_2 \cdot 2H_2O$ (0.5 mmol) was added a methanolic solution of the ligand (0.5 mmol). The resulting parrot-green-colored solution was stirred for 1 h, after which the volume was reduced on a warm water bath. The parrot green product obtained was washed with a small amount of methanol and air-dried. The above product was redissolved in excess warm methanol, and the clear solution was left undisturbed for weeks to give beautiful green needles of the complex, suitable for X-ray diffraction analysis. Crystals were analyzed for composition $CuC_{22}H_{24}N_6O_2Cl_2 \cdot H_2O \cdot CH_3OH$. Anal. Found (Calcd): C, 46.72 (46.89); H, 5.05 (5.10); N, 14.40 (14.27). λ_{max}, nm (log ϵ) (methanol): 758 (2.05), 360 (sh), 277 (4.16), 271 (4.18). μ_{eff} (μ_B) = 1.90. $E_{1/2}$ (V) = +0.584 vs NHE. IR (cm^{-1}, KBr): 3395 ($\nu_{N-H\ amide}$), 3209 ($\nu_{N-H\ benzim}$), 1604 (amide I), 1560 (amide II), 1452 ($\nu_{C=N-C=C}$).

[Cu(NO_3)(GBHA)](NO_3)·0.5H_2O·0.5CH_3OH. This complex was prepared in the same manner as that described for the chloride complex by taking $Cu(NO_3)_2 \cdot 3H_2O$ in place of $CuCl_2 \cdot H_2O$. The green product obtained was washed with methanol, dried in air, and analyzed for composition $CuC_{22}H_{24}N_8O_8 \cdot 0.5H_2O \cdot 0.5CH_3OH$. Anal. Found (Calcd): C, 43.81 (43.79); H, 4.33 (4.38); N, 18.30 (18.17). λ_{max}, nm (log ϵ) (methanol): 782 (1.94), 347 (sh), 277 (4.28), 270 (4.30). μ_{eff} (μ_B) = 2.04. $E_{1/2}$ (V) = +0.599 vs NHE. IR (cm^{-1}, KBr): 3230 ($\nu_{N-H\ amide}$), 3097 ($\nu_{N-H\ benzim}$), 1602 (amide I), 1501 (amide II), 1445 ($\nu_{CdN-C=C}$), 1384 and 821 ($\nu_{O-N-O\ sym\ and\ antisym}$).

[Cu(GBHA)(NCS)](NCS)·3H_2O. To a solution of $CuCl_2 \cdot H_2O$ (0.5 mmol) in methanol was added dropwise a concentrated solution of potassium thiocyanate in methanol. The addition was continued till a precipitate started appearing. At this point the brown solution was centrifuged, and the centrifugate was treated as a standard solution of cupric thiocyanate. This solution was then added to a methanolic solution of the ligand (0.5 mmol). Immediate precipitation of a green

(4) Cescon, L. A.; Day, A. R. *J. Org. Chem.* **1962**, *27*, 581.
(5) Walker, N.; Stuart, D. *Acta Crystallogr.* **1983**, *A39*, 158.
(6) (a) Cromer, D. T.; Waber, J. *International Tables for X-ray Crystallography*; Kynoch Press: Bermingham, U.K., 1974; Vol. IV. (b) Stewart, R. F.; Davidson, E. R.; Simpson, W. T. *J. Chem. Phys.* **1965**, *42*, 3175.
(7) (a) Storm, C. B.; Freeman, C. M.; Butcher, R. J.; Turner, A. H.; Rowan, N. S.; Johnson, F. O.; Sinn, E. *Inorg. Chem.* **1983**, *22*, 678. (b) Spencer, J. T.; Pourian, M. R.; Butcher, R. J.; Sinn, E.; Grimes, R. N. *Organometallics* **1987**, *6*, 335.
(8) Barnes, D. J.; Chapman, R. L.; Vagg, R. S.; Watton, E. C. *J. Chem. Eng. Data* **1978**, *23* (4), 349.

Table 1. Crystal Data and Structure Refinement for $[Cu(GBHA)Cl]Cl{\cdot}H_2O{\cdot}CH_3OH$

empirical formula	$C_{23}H_{30}Cl_2CuN_6O_4$	θ range for data collectn	2.15−27.55°
fw	588.97	limiting indices	$0 \le h \le \mp 27$
temp	293(2) K		$0 \le k \le \mp 13$
wavelength	0.71073 Å		$-26 \le l \le \mp 25$
cryst syst	monoclinic	no. of reflns collected	5831
space group	*C*2/*c*	no. of independent reflns	5703 (R_{int} = 0.0380)
unit cell dimens	a = 26.464 (3) Å	completeness to θ = 27.55°	93.0%
	b = 10.2210 (8) Å	abs correction	integration
	c = 20.444 (2) Å	max and min transm	0.9035 and 0.5525
	α = 90°	refinement method	full-matrix least-squares on F^2
	β = 106.554(7)°	no. of data/restraints/params	5703/3/372
	γ = 90°	goodness-of-fit on F^2	1.031
vol, *Z*	5300.7(9) Å^3, 8	final *R* indices[a] [$I > 2\sigma(I)$]	R1 = 0.0555
density(calcd)	1.476 Mg/m^3		wR2 = 0.1158
abs coeff	1.067 mm^{-1}	*R* indices[a] (all data)	R1 = 0.1073
F(000)	2440		wR2 = 0.1357
cryst size	0.10 × 0.76 × 0.42 mm	largest diff peak and hole	+0.360 and −0.419 e Å^{-3}

[a] $R1 = \sum|(F_o - F_c)|/\sum F_o$. $wR2 = \sum|(F_o - F_c)|w^{1/2}/\sum F_o w^{1/2}$. $w = \sigma(F)^2$.

Table 2. Atomic Coordinates (×10^4) and Equivalent Isotropic Displacement Parameters (Å^2 × 10^3) for $[Cu(GBHA)Cl]Cl{\cdot}H_2O{\cdot}CH_3OH$

	x	*y*	*z*	*U*(eq)[a]
Cu	1671(1)	331(1)	5091(1)	35(1)
Cl(1)	2500(1)	485(1)	5856(1)	54(1)
Cl(2)	464(1)	−4154(2)	6074(1)	82(1)
O(1)	1198(1)	1164(3)	4177(1)	47(1)
O(1W)	446(3)	−4381(5)	3418(3)	96(2)
O(1M)	820(3)	−6069(10)	2640(3)	176(3)
O(2)	1093(1)	−1111(3)	5176(2)	47(1)
N(1A)	1372(1)	1494(3)	5652(2)	34(1)
N(2A)	1040(2)	3198(5)	6050(2)	51(1)
N(3A)	701(2)	2854(4)	4324(2)	46(1)
N(1B)	1946(1)	−792(3)	4483(2)	36(1)
N(2B)	2177(1)	−2461(4)	3954(2)	44(1)
N(3B)	1080(2)	−2856(4)	4507(2)	44(1)
C(1M)	1299(3)	−6338(11)	2878(5)	153(4)
C(1A)	1462(2)	72(5)	6690(2)	56(1)
C(2A)	1380(2)	83(7)	7332(3)	75(2)
C(3A)	1180(2)	1178(9)	7573(3)	84(2)
C(4A)	1049(2)	2298(7)	7201(3)	74(2)
C(5A)	1135(2)	2276(5)	6557(2)	46(1)
C(6A)	1339(2)	1203(4)	6308(2)	39(1)
C(7A)	1189(2)	2698(4)	5520(2)	39(1)
C(8A)	1119(2)	3421(4)	4866(2)	51(1)
C(9A)	773(2)	1755(5)	4012(2)	44(1)
C(10A)	318(2)	1256(5)	3450(2)	55(1)
C(11A)	230(2)	−192(5)	3559(2)	56(1)
C(1B)	2369(2)	952(4)	3931(2)	43(1)
C(2B)	2649(2)	1116(5)	3466(2)	54(1)
C(3B)	2793(2)	59(5)	3135(3)	64(2)
C(4B)	2665(2)	−1206(5)	3250(3)	60(1)
C(5B)	2378(2)	−1373(4)	3719(2)	40(1)
C(6B)	2232(2)	−318(4)	4051(2)	36(1)
C(7B)	1922(2)	−2087(4)	4405(2)	37(1)
C(8B)	1649(2)	−3011(4)	4743(3)	47(1)
C(9B)	839(2)	−1915(4)	4753(2)	42(1)
C(10B)	248(2)	−1831(5)	4490(3)	50(1)
C(11B)	83(2)	−480(5)	4219(2)	49(1)

[a] *U*(eq) is defined as one-third of the trace of the orthogonalized $\mathbf{U}_{ij}$ tensor (hydrogens excluded).

product was observed. The precipitate was filtered off, washed with methanol, dried, and analyzed for composition $CuC_{24}H_{24}N_8O_2S_2{\cdot}3H_2O$. Anal. Found (Calcd): C, 45.60 (45.18); H, 4.67 (4.71); N, 17.72 (17.57). λ_{max}, nm (log ϵ) (methanol): 740 (2.18), 382 (3.03), 278 (4.10), 271 (4.17). μ_{eff} (μ_B) = 2.01. $E_{1/2}$ (V) = +0.621 vs NHE. IR (cm^{-1}, KBr): 3276 ($\nu_{N-H\ amide}$), 3125 ($\nu_{N-H\ benzim}$), 1639 (amide I), 1546 (amide II), 1455 ($\nu_{C=N-C=C}$), 2100 ($\nu_{C\equiv N}$), 800 (ν_{C-S}).

$[Cu^I(NO_3)(GBHA)]{\cdot}0.75CH_3OH$. To a methanolic solution (10 mL) of GBHA (0.5 mmol) was added a methanolic solution (5 mL) of $Cu(NO_3)_2{\cdot}3H_2O$ (0.5 mmol). The resulting parrot green solution was stirred for 1 h in a septum-sealed three-neck flask. A solution of quinol (0.5 mmol) was prepared in methanol (10 mL). High-purity dry nitrogen was then bubbled through both the solutions for 30 min. The quinol solution was then transferred under nitrogen, via a double end needle, to the copper(II) complex solution. An immediate color change from green to pale yellow was observed. Stirring for 10−15 min resulted in a white solid that was filtered off, washed several times with methanol, and dried in vacuo. Anal. Found for $CuC_{22}H_{24}N_7O_5{\cdot}0.75CH_3OH$ (Calcd): C, 49.63 (49.32); H, 4.77 (4.88), N, 17.61 (17.70). $E_{1/2}$ (V) = +0.622 vs NHE. IR (cm^{-1}, KBr): 3275 ($\nu_{N-H\ amide}$), 3195 ($\nu_{N-H\ benzim}$), 1653 (amide I), 1538 (amide II), 1459 ($\nu_{C=N-C=C}$), 1384 and 821 ($\nu_{O-N-O\ sym\ and\ antisym}$). ^{1}H NMR of freshly precipitated $[Cu^I(NO_3)(GBHA)]$ (slightly wet with methanol) in d_6-DMSO: δ (ppm) = 1.54 (quin, br, 4H), 2.21 (t, br, 4H), 4.73 (d, br, 4H), 7.30−7.86 (m, br, 8H), 8.83 (t, br, 2H$_{amide\ NH}$).

Results and Discussion

Description of the Crystal Structure. The crystal structure of the complex $[CuCl(GBHA)]Cl{\cdot}H_2O{\cdot}CH_3OH$ is shown in Figures 3 and 4. The crystals are stable in mother liquor only and tend to become opaque when taken out. Crystals have the space group *C*2/*c* of a monoclinic system.

The coordination environment around the copper atom is pentacoordinate consisting of two benzimidazolyl nitrogen atoms, two amide carbonyl oxygen atoms, and a chloride ion. The structure has the appearance of a trigonal bipyramid in which equatorial positions are occupied by a Cl atom and amide carbonyl oxygen atoms O(1) and O(2) and the axial positions by benzimidazole imine nitrogen atoms N(1A) and N(1B). Cu−N bond distances of 1.967 Å (Cu−N(1A)) and 1.977 Å (Cu−N(1B)) are in the range found for similar benzimidazole- and imidazole-ligated compounds.[9] Cu−O bond distances of 2.111 Å (Cu−O(1)) and 2.166 Å (Cu−O(2)) are considerably longer than those reported in the literature for amide carbonyl coordination.[10]

In pentacoordinated systems, the actual geometry of the complex can be described by a structural index parameter τ[9e] such that $\tau = \beta - \alpha/60°$, where β and α are the two largest angles ($\beta > \alpha$). According to this model, out of the equatorial ligands (A, D, E), A is chosen such that the Cu−A bond length is longer than Cu−D/E and A should not be any one of the four donor atoms forming the two largest angles. Thus, the geometric parameter τ is applicable to pentacoordinated structures as an index of the degree of trigonality, within the structural continuum between trigonal bipyramidal (TBP) ($\beta - \alpha = 60°$, $\tau = 1$) and square pyramidal ($\beta - \alpha = 0°$, $\tau = 0$). The complex

Table 3. Bond Lengths (Å) and Angles (deg) for [Cu(GBHA)Cl]Cl·H_2O·CH_3OH

Cu−N(1A)	1.967(3)	Cu−N(1B)	1.977(3)
Cu−O(1)	2.111(3)	Cu−O(2)	2.166(3)
Cu−Cl(1)	2.3082(12)	O(1)−C(9A)	1.235(5)
O(1M)−C(1M)	1.253(9)	O(2)−C(9B)	1.243(5)
N(1A)−C(7A)	1.322(5)	N(1A)−C(6A)	1.399(5)
N(2A)−C(7A)	1.354(6)	N(2A)−C(5A)	1.370(6)
N(3A)−C(9A)	1.331(6)	N(3A)−C(8A)	1.447(6)
N(1B)−C(7B)	1.333(5)	N(1B)−C(6B)	1.402(5)
N(2B)−C(7B)	1.345(5)	N(2B)−C(5B)	1.376(6)
N(3B)−C(9B)	1.329(6)	N(3B)−C(8B)	1.453(6)
C(1A)−C(6A)	1.382(6)	C(1A)−C(2A)	1.389(7)
C(2A)−C(3A)	1.387(9)	C(3A)−C(4A)	1.363(9)
C(4A)−C(5A)	1.400(7)	C(5A)−C(6A)	1.382(6)
C(7A)−C(8A)	1.491(6)	C(9A)−C(10A)	1.498(6)
C(10A)−C(11A)	1.524(7)	C(11A)−C(11B)	1.535(6)
C(1B)−C(2B)	1.372(6)	C(1B)−C(6B)	1.389(6)
C(2B)−C(3B)	1.384(7)	C(3B)−C(4B)	1.374(7)
C(4B)−C(5B)	1.394(6)	C(5B)−C(6B)	1.386(5)
C(7B)−C(8B)	1.474(6)	C(9B)−C(10B)	1.504(6)
C(10B)−C(11B)	1.506(6)		

N(1A)−Cu−N(1B)	176.89(13)	N(1A)−Cu−O(1)	92.12(12)
N(1B)−Cu−O(1)	84.77(12)	N(1A)−Cu−O(2)	87.41(12)
N(1B)−Cu−O(2)	92.87(13)	O(1)−Cu−O(2)	95.21(12)
N(1A)−Cu−Cl(1)	91.51(10)	N(1B)−Cu−Cl(1)	90.92(10)
O(1)−Cu−Cl(1)	141.46(10)	O(2)−Cu−Cl(1)	123.28(9)
C(9A)−O(1)−Cu	134.7(3)	C(9B)−O(2)−Cu	130.5(3)
C(7A)−N(1A)−C(6A)	106.0(3)	C(7A)−N(1A)−Cu	128.9(3)
C(6A)−N(1A)−Cu	125.1(3)	C(7A)−N(2A)−C(5A)	108.3(4)
C(9A)−N(3A)−C(8A)	121.5(4)	C(7B)−N(1B)−C(6B)	106.5(3)
C(7B)−N(1B)−Cu	129.6(3)	C(6B)−N(1B)−Cu	123.9(3)
C(7B)−N(2B)−C(5B)	109.2(4)	C(9B)−N(3B)−C(8B)	121.2(4)
C(6A)−C(1A)−C(2A)	116.9(6)	C(3A)−C(2A)−C(1A)	121.3(6)
C(4A)−C(3A)−C(2A)	122.8(5)	C(3A)−C(4A)−C(5A)	115.3(6)
N(2A)−C(5A)−C(6A)	105.9(4)	N(2A)−C(5A)−C(4A)	131.1(5)
C(6A)−C(5A)−C(4A)	123.0(5)	C(1A)−C(6A)−C(5A)	120.6(4)
C(1A)−C(6A)−N(1A)	130.6(4)	C(5A)−C(6A)−N(1A)	108.8(4)
N(1A)−C(7A)−N(2A)	111.1(4)	N(1A)−C(7A)−C(8A)	126.1(4)
N(2A)−C(7A)−C(8A)	122.7(4)	N(3A)−C(8A)−C(7A)	111.1(4)
O(1)−C(9A)−N(3A)	121.7(4)	O(1)−C(9A)−C(10A)	120.8(4)
N(3A)−C(9A)−C(10A)	117.5(4)	C(9A)−C(10A)−C(11A)	109.9(4)
C(10A)−C(11A)−C(11B)	113.7(4)	C(2B)−C(1B)−C(6B)	117.1(4)
C(1B)−C(2B)−C(3B)	121.5(5)	C(4B)−C(3B)−C(2B)	122.3(5)
C(3B)−C(4B)−C(5B)	116.2(4)	N(2B)−C(5B)−C(6B)	105.6(4)
N(2B)−C(5B−C(4B)	132.8(4)	C(6B)−C(5B)−C(4B)	121.6(4)
C(5B)−C(6B)−C(1B)	121.2(4)	C(5B)−C(6B)−N(1B)	108.4(4)
C(1B)−C(6B)−N(1B)	130.4(4)	N(1B)−C(7B)−N(2B)	110.3(4)
N(1B)−C(7B)−C(8B)	126.4(4)	N(2B)−C(7B)−C (8B)	123.3(4)
N(3B)−C(8B)−C(7B)	112.0(4)	O(2)−C(9B)−N(3B)	121.2(4)
O(2)−C(9B)−C(10B)	120.8(4)	N(3B)−C(9B)−C(10B)	118.0(4)
C(9B)−C(10B)−C(11B)	110.3(4)	C(10B)−C(11B)−C(11A)	112.3(4)

[CuCl(GBHA)]Cl·H_2O·CH_3OH has a τ value of 0.591, indicating a distortion from perfect TBP toward distorted TBP. This complex does not fit the above-described model fully, since the Cu−O(2) (Cu−A) bond length of 2.166 Å is shorter than the Cu−Cl(1) (Cu−D/E) bond length of 2.3082 Å. This observed Cu−Cl(1) bond length is in a range similar to that observed for similar pentacoordinated Cu(II) compounds.[9f,i,11] This coordinated Cl atom is also hydrogen bonded to the benzimidazole NH of the neighboring complex molecule. Equatorial bond angles deviate largely from the expected value of 120°, the largest deviation being 24.79°, whereas N(1A)−Cu−N(1B) is 176.89(13)°. The sum of equatorial bond angles at Cu is 359.95°, showing that the metal ion is essentially in the mean plane of the equatorial donors.

The crystal consists of layers of [CuCl(GBHA)]Cl·H_2O·CH_3-OH stacked over each other, held together by $NH_{amide}\cdots O_{water}$ and $NH_{amide}\cdots O_{MeOH}$ interactions, whereas molecules within the layers are H-bonded to each other via $NH_{benzim}\cdots$Cl bonds.

(9) (a) Tandon, S. S.; Thompson, L. K.; Bridson, J. N.; Dewan, J. C. *Inorg. Chem*. **1994**, *33* (1), 54. (b) Addison, A. W.; Burke, P. J.; Henrick, K.; Rao, T. N.; Sinn, E. *Inorg. Chem*. **1983**, *22*, 3645. (c) Hendricks, H. M. J.; Birker, P. J. M. W. L.; Rijn, J. V.; Verschoor, G. C.; Reedijk, J. *J. Am. Chem. Soc*. **1982**, *104* (13), 3607. (d) Reitmeijer, F. J.; Birker, P. J. M. W. L.; Gorter, S.; Reedijk, J. *J. Chem. Soc., Dalton Trans*. **1982**, 1193. (e) Rao. T. N.; Addison, A. W. *J. Chem. Soc., Dalton Trans*. **1984**, 1349. (f) Rijn, J. V.; Driessen, W. L.; Reedijk, J.; Lehn, J. M. *Inorg. Chem*. **1984**, *23*, 3584. (g) Birker, P. J. M. W. L.; Godefroi, E. F.; Helder, J.; Reedijk, J. *J. Am. Chem. Soc*. **1982**, *104*, 7556. (h) Monzani, E., Quinti, L.; Perotti, A.; Casella, L.; Gulloti, M.; Randaccio, L.; Geremia, S.; Nardin, G.; Faleschini, P.; Tabbi, G. *Inorg. Chem*. **1998**, *37*, 553. (i) Birker, P. J. M. W. L.; Helder, J.; Henkel, G.; Krebs, B.; Reedijk, J. *Inorg. Chem*. **1982**, *21*, 357. (j) Dagdigian, J. V.; Mckee, V.; Reed, C. A. *Inorg. Chem*. **1982**, *21* (4), 1332. (k) Juen, S.; Yishen, Z. *Inorg. Chim. Acta* **1989**, *162*, 29.

(10) (a) Lloret, F.; Julve, M.; Faus, J.; Journax, Y.; Levisalles, M. P.; Jeannin, Y. *Inorg. Chem*. **1989**, *28*, 3702. (b) Lloret, F.; Julve, M.; Faus, J.; Ruiz, R.; Castro, I.; Mollar, M.; Levisalles, M. P. *Inorg. Chem*. **1992**, *31*, 784. (c) Frances, L.; Julve, M.; Real, J.; Faus, J.; Ruiz, R.; Mollar, M.; Castro, I.; Bois, C. *Inorg. Chem*. **1992**, *31*, 2956. (d) Lloret, F.; Sletten, J.; Ruiz, R.; Julve, M.; Faus, J.; Verdaguer, M. *Inorg. Chem*. **1992**, *31*, 778. (e) Sangeetha, N. R.; Baradi, K.; Gupta, R.; Pal, C. K.; Manivannan, V.; Pal, S. *Polyhedron* **1999**, *18*, 1425.

(11) Vezzosi, I. M.; Antolini, L. *Inorg. Chim. Acta* **1984**, *85*, 155.

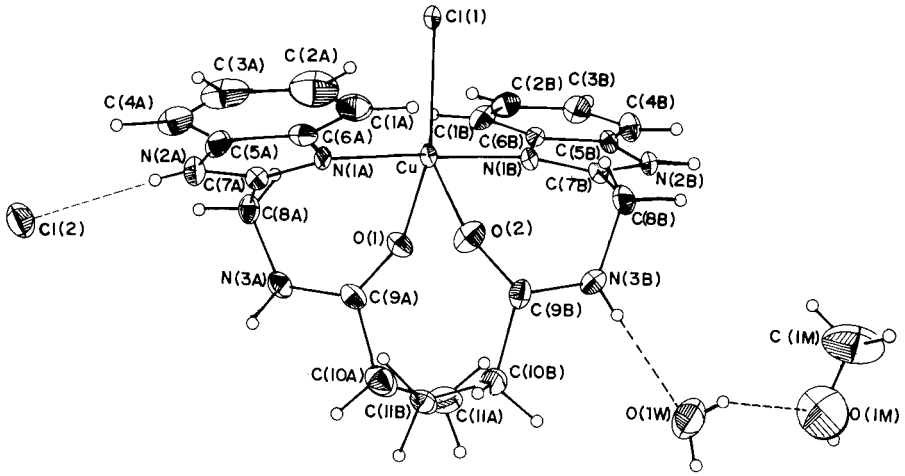

Figure 3. ORTEP projection of [Cu(GBHA)Cl]Cl·H_2O·CH_3OH showing the atomic numbering scheme.

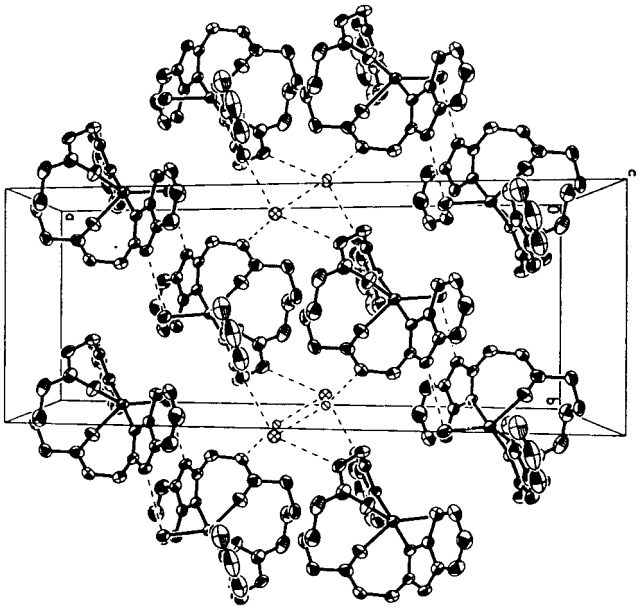

Figure 4. Stereo drawing of the unit cell contents of [Cu(GBHA)Cl]-Cl·H_2O·CH_3OH.

^{1}H NMR, Electronic Spectroscopy, and Cyclic Voltammetry. The electronic spectra of all the complexes were measured in methanol. UV bands at 272 and 279 nm are observed for the free ligand GBHA. These bands are characteristic of the benzimidazole group and arise from a $\pi \rightarrow \pi^*$ transition.[9h] All the complexes display a broad d−d band in the region 740−790 nm (Figure 5A) characteristic of tetragonal geometry. A shoulder due to a LMCT (imidazole $\pi_1 \rightarrow Cu^{2+}$) band in the region 340−390 nm is also observed.[9h] The UV band in the complexes corresponding to a $\pi \rightarrow \pi^*$ transition shows enhanced absorption as indicated by their extinction coefficients.

The ^{1}H NMR spectrum of the free ligand GBHA (Figure 6a) shows signals for aliphatic and aromatic protons with theoretically predicted splittings. A symmetrical multiplet in the range 7.15−7.49 ppm arises due to benzimidazole ring protons characteristic of an AA′BB′ pattern. A triplet at 8.44 ppm arises due to amide NH protons (coupled with adjacent CH_2 protons (c)) (J = 5.58 Hz). These CH_2 protons (c) also give rise to a doublet at 4.54 ppm due to coupling with the adjacent amide NH proton (J = 5.5 Hz). Benzimidazole NH protons give a broad signal at 12.07 ppm. In the Cu(I) complex the aromatic ligand proton resonances are observed in two groups with a 1:3 proton ratio (Figure 6b), unlike in GBHA where both the signals have the same proton integration. In the Cu(I) complex the three aromatic protons (H_5, H_6, H_7) remain at the chemical shift close to that observed in the free ligand GBHA, while proton H_4 is shifted downfield, being nearest to the imidazole N atom bound to Cu(I).[12] The signals are slightly broadened possibly due to the presence of trace Cu(II) ions.

All the complexes display a quasi-reversible redox wave (Figure 7) due to the Cu(II)/Cu(I) process. Anodic shifts in $E_{1/2}$ values indicate the retention of the anion in the coordination sphere of Cu(II). The $E_{1/2}$ values vary anodically in the order $Cl^- < NO_3^- < SCN^-$. This indicates that bound thiocyanate destabilizes the Cu(II) state while bound chloride stabilizes it. The $E_{1/2}$ value for the copper(I) complex [$Cu^I(NO_3)$(GBHA)] was found to be +0.622 V vs NHE. No redox wave associated with bound quinone or quinol was found in its cyclic voltammogram. When calculated against NHE, the $E_{1/2}$ values of the present series of Cu(II) complexes turn out to be quite positive as compared to those of other Cu(II) complexes with benzimidazole[13]-based ligands (+0.00 to +0.446 V)[9h,13a,b] and some amide-based complexes.[14] Binding of amide N, preferably in deprotonated form, is known to stabilize copper in higher oxidation states (+2, +3), thus cathodically shifting the reduction potential values.[15] In contrast the binding of an amide carbonyl oxygen apparently has a destabilizing effect on Cu(II), leading to relatively a high anodic redox potential for this series of complexes.

EPR, Magnetic, and IR Spectral Properties. X-band EPR spectra of the Cu(II) complexes were recorded in DMSO at liquid nitrogen temperature. Spectra typically indicate a $d_{x^2-y^2}$ ground state ($g_{\|} > g_{\perp} > 2.0023$). For [CuCl(GBHA)]Cl $g_{\|}$ = 2.33, $g_{\perp}$ = 2.07, and $A_{\|}$ = 145 G. For $Cu(SCN)_2$(GBHA) $g_{\|}$ = 2.30, $g_{\perp}$ = 2.05, and $A_{\|}$ = 165 G. The EPR spectra of these complexes also suggest a change in geometry to a tetragonal

(12) Thompson. L, K.; Ramaswamy, B. S.; Seymour, E. A. *Can. J. Chem.* **1977**, *55*, 878.
(13) (a) Nakao, Y.; Onoda, M.; Sakurai, T.; Nakahara, A.; Kinoshita, L.; Ooi, S. *Inorg. Chim. Acta* **1988**, *151*, 55. (b) Addison, A. W.; Hendricks, H. M. J.; Reedijk, J.; Thompson, L. K. *Inorg. Chem.* **1981**, *20* (1), 103. (c) Sivagnanam, U.; Palaniandavar, M. *J. Chem. Soc., Dalton Trans*. **1994**, 2277. (d) Palaniandavar, M.; Pandiyan, T.; Laxminarayan, M.; Manohar, H. *J. Chem. Soc., Dalton Trans.* **1995**, 457. (e) Sakurai, T.; Oi, H.; Nakahara, A. *Inorg. Chim. Acta* **1984**, *92*, 131.
(14) Patra, A. K.; Ray, M.; Mukherjee, R. *J. Chem. Soc., Dalton Trans.* **1999**, 2461.
(15) Anson, F.C.; Collins, T.J.; Richmond, T.G.; Santarsiero, B.D.; Toth, J.E.; Treco, G.R. T. *J. Am. Chem. Soc.* **1987**, *109*, 2974.

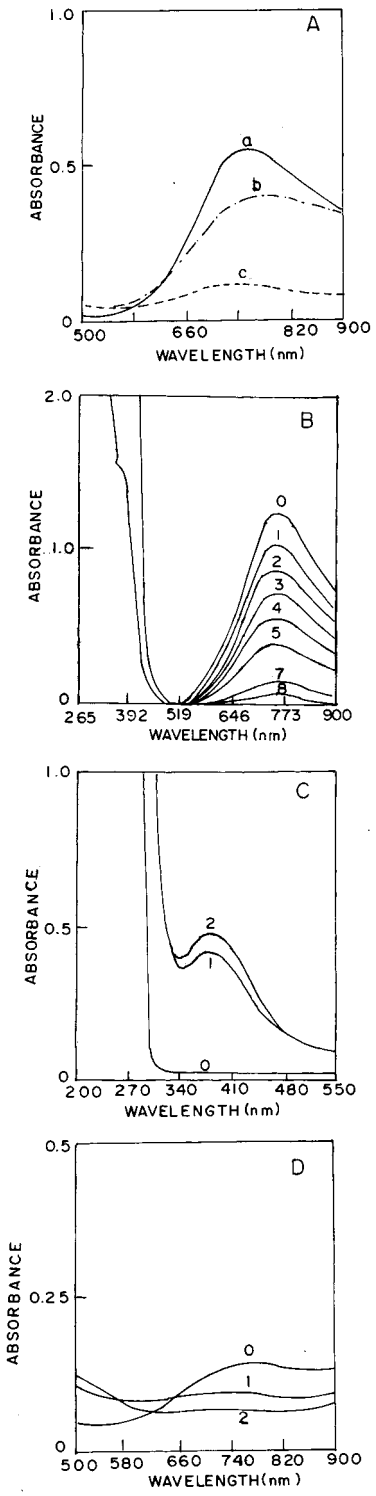

Figure 5. (A) Visible spectra of Cu(II) complexes in methanol: (a) $Cu(GBHA)Cl_2$, (b) $Cu(GBHA)(NO_3)_2$, (c) $Cu(GBHA)(SCN)_2$. (B) Visible spectra of a 7.8 mM solution of $Cu(GBHA)(NO_3)_2$ in a 2:8 DMSO−CH_3CN solution (curve 0) and $Cu(GBHA)(NO_3)_2$ in the presence of quinol (curves 1−8). (C) UV spectra of a catechol solution (30 mM, air-saturated MeOH) (curve 0) and a new band generated in the presence of a $Cu(GBHA)(NO_3)_2$ solution (curves 1 and 2). (D) Visible spectra of a $Cu(GBHA)(NO_3)_2$ solution (1.1 mM, MeOH) (curve 0) and $Cu(GBHA)(NO_3)_2$ in the presence of catechol (curves 1 and 2).

site on going from the solid to the solution state.[14] However, this tetragonal geometry is severely distorted as all of them show less than four $g_{\|}$ lines and a broadening of the $g_{\perp}$ line. Such a broadening of the $g_{\perp}$ component is indicative of lower symmetry

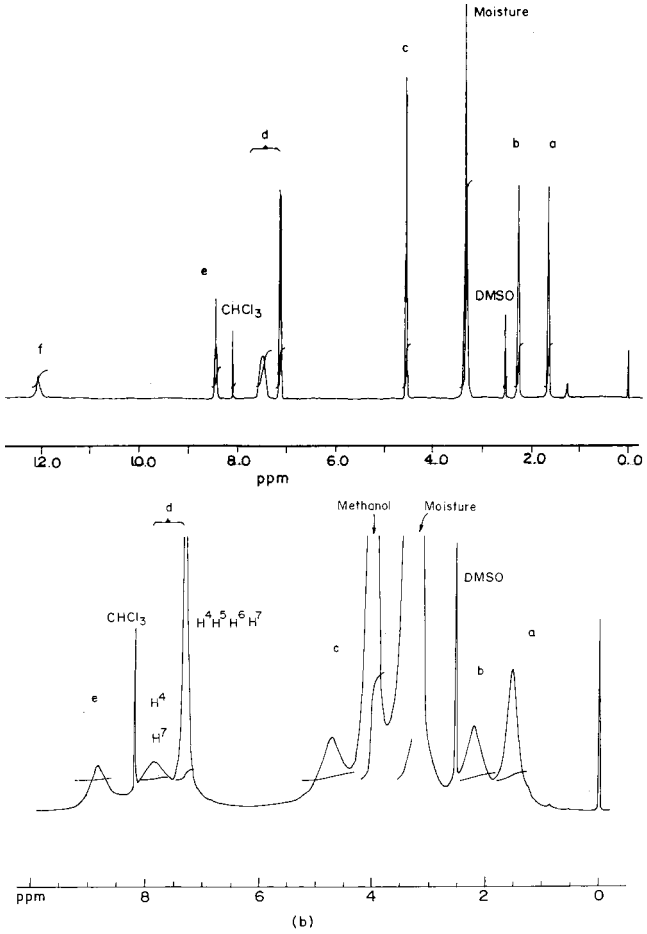

Figure 6. ^1H NMR (300 MHz) spectra of (a) GBHA and (b) Cu(GBHA)NO_3 in d_6-DMSO.

manifesting itself through a rhombic splitting.[16] Moreover, the values of the hyperfine coupling constant $A_{\|}$ are quite low in comparison to the normal range found for other copper(II) complexes,[17] implying a marked tetrahedral distortion of the tetragonal site.[18] No nitrogen super hyperfine splitting could be observed.

The magnetic susceptibilities of the Cu(II) complexes were determined in the solid state at room temperature. μ_{eff} values lie within the range normally found for other Cu(II) complexes.[19]

The free ligand GBHA has characteristic IR bands at 1635, 1539, and 1448 cm^{-1}. These are assigned to amide I (mainly $\nu_{C=O\ amide}$ stretch), amide II (mainly $\nu_{C=N\ amide}$ stretch),[19] and benzimidazole $\nu_{C=N-C=C}$[20] stretching frequencies, respectively. ν_{N-H} stretching bands arise at 3296 and 3185 cm^{-1} due to the amide NH and benzimidazole NH, respectively. On complexation a decrease in the amide I stretching frequencies and an increase in the amide II stretching frequencies have been observed, which is in accordance with the coordination of the

(16) (a) Weser, U.; et al. *Biochim. Biophys. Acta* **1971**, *243*, 203. (b) Blumberg, W. E.; Peisach, J. *J. Biol. Chem.* **1965**, *240*, 870.
(17) Malmstrom, B. C.; Vamngard, T. *J. Mol. Biol.* **1960**, *2*, 118.
(18) (a) Seebauer, E. C.; Duliba, E. P.; Gennis, R. B.; Belford, R. L. *J. Am. Chem. Soc.* **1983**, *105*, 4926. (b) Sakaguchi, U.; Addisson, A. W. *J. Chem. Soc., Dalton Trans.* **1979**, 600. (c) Batra, G.; Mathur, P. *Inorg. Chem.* **1992**, *31*, 1575.
(19) (a) Nonoyama, M.; Yamasaki, K. *Inorg. Chim. Acta* **1969**, *3*, 585. (b) Nonoyama, M.; Yamasaki, K. *Inorg. Chim. Acta* **1973**, *7*, 676. (c) Nonoyama, M.; Yamasaki, K. *Inorg. Chim. Acta* **1971**, *5*, 124. (d) Shazly, M. F.; El-Dissowky, A.; Salem, T.; Osman, M. *Inorg. Chim. Acta* **1980**, *40*, 1.
(20) Mathur, P.; Crowder, M.; Dismukes, G. C. *J. Am. Chem. Soc.* **1987**, *109*, 5227.

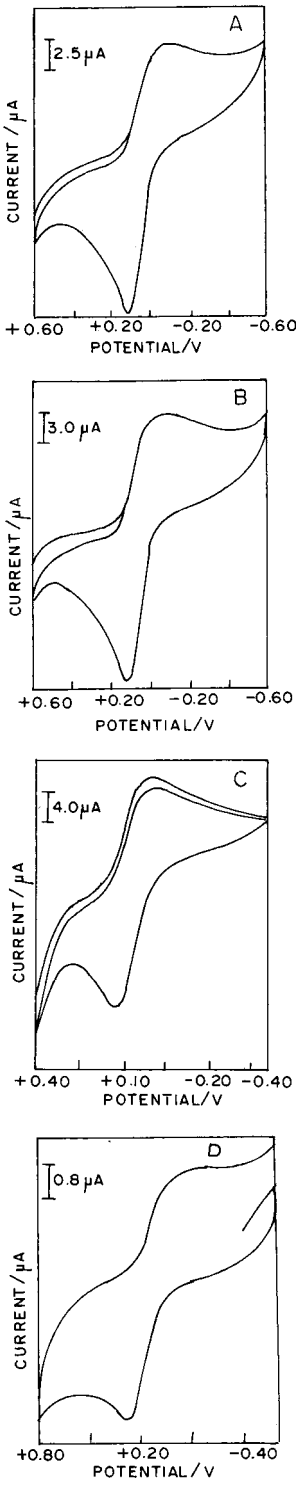

Figure 7. Cyclic voltammograms of (A) $Cu(GBHA)Cl_2$, (B) $Cu(GBHA)(NO_3)_2$, (C) $Cu(GBHA)(SCN)_2$, and (D) $Cu(GBHA)NO_3$ in a 2:8 DMSO−CH_3CN solution at a scan rate of 100 mV/s.

ligand through an amide carbonyl oxygen.[19a] Shifts in N−H stretching frequencies are due to the hydrogen bonding between the benzimidazole NH and the coordinated Cl atom of the neighboring complex molecule and between the amide NH and a water molecule. A broad band in the range 3250−3400 cm^{-1} (ν_{O-H} stretch) indicates the presence of water molecules as the solvent of crystallization. Characteristic stretching frequencies for the coordinated anions are also observed. Bands at 2100 and 800 cm^{-1} in the thiocyanato complex are assigned to $\nu_{C=N}$ and ν_{C-S} stretching of the thiocyanate group. This shows coordination of the thiocyanato group through the N atom.[19b] The nitrate complex shows bands at 1384 and 828 cm^{-1} due to $\nu_{O-N-O\ sym}$ and $\nu_{O-N-O\ antisym}$ stretching of the coordinated nitrate group.[21] The IR spectrum of the Cu(I) complex $[Cu(NO_3)(GBHA)]$ also displays bands at the same positions due to the nitrate group, indicating its coordination to Cu(I).

On the basis of the above studies, it is concluded that the nitrate and thiocyanate complexes would have the same stereochemistry as that of the chloride complex, with varying degrees of the trigonality index.

Electron Exchange Reaction between $[Cu(NO_3)_2(GBHA)]$ and *o*/*p*-Dihydroxybenzenes. The reduction of $[Cu(NO_3)_2(GBHA)]$ by quinol was studied spectrophotometrically under anaerobic conditions. A 7.8 mM $[Cu(NO_3)_2(GBHA)]$ solution was prepared in a 1:9 DMSO−CH_3CN solution. Dry nitrogen was bubbled through this septum-sealed solution for 1/2 h. A spectrum of the above complex in this solvent system displays a broad band centered at 747 nm ($\epsilon = 154\ M^{-1}\ cm^{-1}$). A 35.5 mM solution of quinol was prepared in a 1:9 DMSO−CH_3CN solution, and dry nitrogen was also bubbled through this septum-sealed solution. A 0.04 mL sample of the above quinol solution was added to 2.0 mL of the Cu(II) complex solution in a septum-sealed quartz cuvette, with the help of an airtight syringe. The reduction of Cu(II) to Cu(I) was followed by observing the decrease in the optical density of the band centered at 747 nm. The same volume of quinol was added periodically, and the decrease in band intensity was monitored till the 747 nm band almost vanished (Figure 5B). At this point the Cu:quinol stoichiometry was 1:0.75. The color of the solution faded to light yellow, indicating the disappearance of the Cu(II) species in the solution. The above yellow solution could be reoxidized by atmospheric oxygen to give a green solution, restoring the wavelength maximum at 747 nm. The same experiment was repeated with simple $Cu(NO_3)_2$ in the absence of the ligand GBHA. No fading of the light blue color to yellow was observed. Instead the color changed to green.

Oxidation of Catechol by $[Cu(NO_3)_2(GBHA)]$. This experiment was also followed spectrophotometrically. The solvent employed for this experiment was methanol-saturated with atmospheric oxygen. A 30 mM solution of catechol in this solvent displays no band in the region 300−900 nm. A solution of $[Cu(NO_3)_2(GBHA)]$ (3.3 mM) was also prepared in air-saturated methanol. To a 2.0 mL catechol solution (containing 6×10^{-2} mmol of catechol) in a quartz cuvette was added 1.0 mL of the Cu(II) solution (containing 3.3×10^{-3} mmol of $[Cu(NO_3)_2(GBHA)]$). The absorption spectrum in the region of 300−900 nm was immediately scanned (Figure 5C(1),D(1)). Scanning was continued after every 5 min. Parts C(2) and D(2) of Figure 5 depict the fate of the solution after 15 min. In this case not only was the reduction in the d−d band intensity (Figure 5D) observed but also the simultaneous appearance of a new band at 377 nm (Figure 5C) was detected which grew with time. This new band is assigned to *o*-benzoquinone being formed as a result of catechol oxidation.[22]

The observed reduction of the Cu(II) complex to the Cu(I) complex with simultaneous oxidation of quinol and catechol

(21) (a) Gatehouse, B. M.; Livingstone, S. E.; Nyholm, R. S. *J. Chem. Soc*. **1957**, Part 4, 4222. (b) Menage, S.; Que, L., Jr. *Inorg. Chem*. **1990**, *29*, 4293.
(22) (a) Thomson, R. H. *Naturally Occurring Quinones*, 2nd ed.; Academic Press: London and New York, 1971; pp 48−49. (b) Cooper, S. R.; Koh, Y. B.; Raymond, K. N. *J. Am. Chem. Soc*. **1982**, *104*, 5092.
(23) Soloman, E. I.; Tuczek, F.; Brown, C. A.; Root, D. E. *Chem. Rev*. **1994**, *94* (3), 827.

mimics the *met*-tyrosinase activity of the copper-containing tyrosinase and catecholase enzymes.

Acknowledgment. We gratefully acknowledge financial support from the Department of Science and Technology, India, for Project No. SP/S1/F35/98. One of the authors, M.G., is thankful to the Council of Scientific and Industrial Research, India, for awarding a junior research fellowship.

IC000313V